Available online at www.sciencedirect.com
SCIENCE DIRECT
Molecular & Biochemical Parasitology 148 (2006) 69–78
MOLECULAR & BIOCHEMICAL PARASITOLOGY

Isolation and characterization of mitochondrial ribosomes and ribosomal subunits from *Leishmania tarentolae*

Dmitri A. Maslov[a,*], Manjuli R. Sharma[b], Evelin Butler[a], Arnold M. Falick[c], Mari Gingery[d], Rajendra K. Agrawal[b,e], Linda L. Spremulli[f], Larry Simpson[d]

[a] *Department of Biology, University of California, Riverside, CA 92521, USA*
[b] *Division of Molecular Medicine, Wadsworth Center, NY State Department of Health, Albany, NY 12201, USA*
[c] *Howard Hughes Medical Institute, Mass Spectrometry Laboratory and Department of Molecular and Cell Biology, University of California, Berkeley, CA 94720, USA*
[d] *Department of Microbiology, Immunology and Molecular Genetics, University of California, Los Angeles, CA 90095, USA*
[e] *Department of Biomedical Sciences, State University of New York at Albany, Albany, NY 12201, USA*
[f] *Department of Chemistry, University of North Carolina, Chapel Hill, NC 27599, USA*

Received 30 November 2005; received in revised form 17 February 2006; accepted 28 February 2006
Available online 24 March 2006

Abstract

We have analyzed *Leishmania tarentolae* mitochondrial ribonucleoprotein (RNP) complexes using the 9S small subunit (SSU) rRNA and the 12S large subunit (LSU) rRNA as markers, and have identified a 50S RNP particle as the putative mitochondrial monosome, a 40S particle as the putative LSU and a 30S particle as the putative SSU. These assignments are supported by morphological analysis by cryo-electron microscopy and proteomics analyses by mass spectrometry. The presence of additional rRNA-containing particles complicated the analysis and most likely was the basis for previous difficulties in identification of these ribosomes; thus, in addition to the monosomes and their subunits, there are abundant stable 45S particles (SSU*) containing only 9S rRNA, which may represent homodimers of the SSU or SSU associated with additional proteins, and variable minor amounts of 65S and 70S particles, which represent homodimers of the LSU and SSU*, respectively. These additional rRNA particles might be due to the lengthy mitochondrial isolation and ribosome isolation procedures or may be present in vivo and play yet undetermined roles.

Keywords: *Leishmania tarentolae*; Kinetoplast; Mitochondrial ribosome; Ribonucleoprotein complex; 9S SSU rRNA; 12S LSU rRNA

1. Introduction

The single large mitochondrion in trypanosomes and related organisms contains a large amount of DNA localized in a discrete portion of the organelle termed the kinetoplast. The kinetoplast DNA contains thousands of minicircles and dozens of maxicircles catenated into a giant network. The maxicircle molecules encode 18 subunits of mitochondrial protein complexes and also two unusually small ribosomal RNAs: 12S (LSU) and 9S (SSU) rRNA molecules (reviewed in refs. [1–3]). Expression of many of the protein-coding genes depends on post-transcriptional U-insertion/deletion RNA editing [4–6] that occurs through an enzymatic cleavage-ligation mechanism [7–11]. Direct biochemical proof that the mitochondrion has an active translational system was obtained when mitochondrial-encoded polypeptides for cytochrome *c* oxidase subunit I (COI) and apocytochrome *b* (Cyb) were identified and their N-terminal sequences were found to match those of their respective mRNAs [12,13]. Subsequently, the synthesis of these polypeptides was demonstrated in organello [14] and in vivo [15]. Surprisingly, the synthesis of COI and Cyb was resistant to most known inhibitors of mitochondrial translation in other systems, including chloramphenicol [14,15].

The 12S large subunit (LSU) and 9S small subunit (SSU) trypanosomatid mitochondrial rRNAs are smaller than the mammalian mitochondrial 16S and 12S rRNAs and are much smaller

Abbreviations: CID, collision-induced dissociation; cryo-EM, cryo-electron microscopy; DTT, dithiotreitol; LC, liquid chromatography; LSU, large subunit; MALDI, matrix-assisted laser desorption-ionization; MRP, mitochondrial ribosomal protein; MS, mass spectrometry; rRNA, ribosomal RNA; SSU, small subunit; TOF, time-of-flight

* Corresponding author. Tel.: +1 951 827 6485; fax: +1 951 827 4286.
E-mail address: maslov@ucr.edu (D.A. Maslov).

0166-6851/$ – see front matter © 2006 Elsevier B.V. All rights reserved.
doi:10.1016/j.molbiopara.2006.02.021

than the eubacterial 23S and 16S rRNAs [16,17]. Secondary structure analyses of the 9S and 12S rRNAs indicated that the size reductions are due to missing stem-loop structures in all structural domains of these molecules, especially in the 3′ minor domain of the SSU rRNA and in domains I and III of the LSU rRNA [17–19]. The remaining domains are also drastically reduced in size. Domain V of the LSU rRNA is the best conserved, possibly since this constitutes the functionally important peptidyl transferase center of the ribosome.

The identification and characterization of the mitochondrial ribosomes of trypanosomatids is a major unsolved problem in this field. Chugunov et al. [20] and Hanas et al. [21] reported the presence of 70S ribosomes and a mitochondrial translation system sensitive to chloramphenicol inhibition, similar to that found in eubacterial and mammalian mitochondrial systems. However, these conclusions were not substantiated by further work. Shu and Göringer [22] reported an 80S RNP complex containing small subunit and large subunit ribosomal RNAs in a novel 3:2 ratio in *Trypanosoma brucei*, and Tittawella et al. [23] described a 35S RNP complex with an undefined rRNA ratio in *Crithidia fasciculata*. In this report, we describe the isolation and properties of several rRNP complexes from *Leishmania tarentolae* mitochondria which, based on their characteristic morphologies as well as on RNA and protein contents, have been identified as mitochondrial monosomes and LSU and SSU ribosomal subunits. In addition, we have found several rRNA-containing complexes possibly arising from oligomerization of the subunits and/or their association with additional proteins. It should be noted that these unusual particles may represent artifacts of the mitochondrial isolation and/or ribosome isolation procedures and may not necessarily exist in vivo.

2. Materials and methods

2.1. Cell growth and fractionation

Cultivation of UC strain *L. tarentolae* cells and isolation of the kinetoplast–mitochondrial fraction from hypotonically lysed cells were performed as described previously [24], except for the use of Percoll density gradients (20–35%) instead of Renografin gradients. Isolated mitochondria were resuspended in SoHE buffer containing 0.6 M sorbitol, 100 mM Hepes–KOH, pH 7.0 and 1 mM EDTA, and used immediately.

2.2. Isolation of rRNP complexes

A standard isolation from a 4 to 6 l culture with a cell concentration of approximately 150×10^6 late log phase cells ml^{-1} usually yielded 0.8–1.0 g purified mitochondria (wet weight). The entire material was resuspended in 35 ml of SoHE and incubated on ice with 2 mM puromycin for 30 min. Organelles were pelleted for 5 min at 30,000 × *g*, resuspended in 25 ml of lysis buffer containing 2% dodecyl maltoside (Calbiochem), 50 mM Tris–HCl, pH 7.5, 100 mM KCl, 10 mM $MgCl_2$, 5 mM DTT and 0.1 mM EDTA, and incubated on ice for 40 min. Insoluble material was removed by pelleting at 17,500 rpm (21,700 × *g*) for 30 min in a Type 60Ti rotor. Portions (4 ml) of the cleared lysate were loaded on six 7–30% linear sucrose gradients (32 ml) made with the SGB buffer (50 mM Tris–HCl, pH 7.5, 100 mM KCl, 10 mM $MgCl_2$, 3 mM DTT, 0.1 mM EDTA and 0.05% dodecyl maltoside). Gradients were centrifuged in an SW28 rotor at 19,000 rpm ($RCF_{avg} = 47{,}800 \times g$) for 16 h. Gradients were fractionated by displacement from the bottom using an ISCO Gradient Fractionation System into thirty-six 1 ml fractions.

2.3. Extraction and analysis of mitochondrial ribosomal RNA

Aliquots (50–300 μl) of individual fractions were extracted once with phenol–chloroform after addition of SDS to 1%. Glycogen (Ambion) was added to 100 μg ml^{-1} and the RNA was precipitated with an equal volume of isopropanol at −20 °C. RNA samples were analyzed in 4% polyacrylamide-urea gels. Sedimentation profiles of the 12S and 9S rRNAs were quantified by measuring the integrated optical density (IOD) of fluorescence of individual bands in gels stained with ethidium bromide using the BioChemi Gel Documentation System (UVP). Apparent *S*-values were estimated by comparison with *Escherichia coli* monosomes (70S) and ribosomal subunits (30S and 50S) sedimented in a parallel gradient.

2.4. Re-sedimentation of ribosomal complexes

Ribosomal complexes contained in gradient fractions were recovered by pelleting at 70,000 rpm (200,000 × *g*), resuspended in 100–300 μl of SGB buffer and centrifuged once again on 7–30% sucrose gradients in an SW41 rotor at 20,000 rpm ($RCF_{avg} = 49{,}400 \times g$) for 16 h. The gradients were fractionated into thirty-six 300 μl fractions and analyzed as described above.

2.5. Negative staining electron microscopy

Carbon-coated parlodion support films mounted on copper grids were made hydrophilic immediately before use by high-voltage, alternating current glow-discharge. Samples from sucrose gradient fractions were applied directly onto grids and allowed to adhere for 2.5 min. Grids were rinsed with three drops of distilled water and stained with 1% uranyl acetate for 30 s. Specimens were examined in a Hitachi H-7000 electron microscope at an accelerating voltage of 75 kV. Images were recorded on Kodak electron microscope film 4489.

2.6. Cryo-electron microscopy and image processing

Cryo-EM grids of the 50S complex were prepared according to standard procedures [25]. Data were collected on a Philips FEI (Eindhoven, The Netherlands) Tecnai F20 FEG microscope, equipped with low-dose kit and an Oxford cryo-transfer holder, at a magnification of 50,760-fold between 2.15 and 4.35 μm under focus range. Forty best micrographs were scanned on a Zeiss flatbed scanner, with a step size of 14 μm, corresponding to 2.76 Å on the object scale. Eleven thousand eight hundred and ninety-one good particle images were manually selected from the scanned micrographs, and were subjected to reference-free

alignment and two-dimensional correspondence analysis [26] using SPIDER [27].

2.7. MALDI tandem mass spectrometry (MALDI MS/MS)

Polypeptides from the 65S fraction representing dimerized 40S complexes were partially resolved on a Novex® 8–16% Tris–Glycine–SDS gel (Invitrogen) and stained using Colloidal Coomassie Blue (Invitrogen). The gel lane was divided into 16 slices each containing several closely migrating protein bands. The slices were destained using a solution of 25 mM ammonium bicarbonate, 50% acetonitrile. In-gel protein digestions were performed with trypsin (Promega, 200 ng per digest) in a solution of 25 mM ammonium bicarbonate, 1 mM $CaCl_2$ for 14 h at 37 °C. The proteolytic products were recovered by extraction with 5% trifluoroacetic acid, 50% acetonitrile (twice), followed by extraction with 5% formic acid, 50% acetonitrile (twice) in a Branson Ultrasonic Cleaner water bath. The peptides were purified with $ZipTip_{C18}$ (Millipore) as recommended by the manufacturer. The collected peptides in each sample were fractionated using a Magic C18 reverse-phase HPLC column (0.1 mm × 150 mm) mounted on a Paradigm HPLC (Michrom BioResources). The elution was done using a 9–60% gradient of acetonitrile in aqueous 1% formic acid and 0.005% heptafluorobutyric acid at a flow rate of 1 μl min^{-1} for 35 min. Fractions were collected automatically with a Probot (Dionex). Matrix (7 g l^{-1} of α-cyano-4-hydroxycinnamic acid in 70% acetonitrile) was added continuously to the column effluent at approximately 2 μl min^{-1}. Samples were collected directly onto the MALDI target plate at 20 s per spot. Approximately 25 sample spots were collected per gel band.

MALDI TOF/TOF mass spectrometric measurements [28] were performed on an Applied Biosystems (Foster City, CA) 4700 Proteomics Analyzer. Normal reflector spectra were acquired first to identify the masses of the peptides of interest. MS/MS CID spectra were acquired manually on each selected peptide, using air as the collision gas and 1 keV (lab frame) collision energy. MS/MS spectra were interpreted manually and the derived sequences were searched using the *Leishmania major* GeneDB BLAST program (http://www.genedb.org/genedb/leish/blast.jsp) to identify homologs of the *L. tarentolae* proteins.

2.8. Liquid chromatography tandem mass spectrometry (LC MS/MS)

The combined 45S and 50S fraction material obtained after sucrose gradient centrifugation was partially purified using ion-exchange chromatography on HiTrap Q Sepharose (Amersham Biosciences). Elution was performed with a 100–1000 mM gradient of KCl in the SGB buffer. The particles from the pooled peak fractions were recovered by pelleting, resuspended in 25 mM ammonium bicarbonate and digested with trypsin. Approximately 5 μg of the ribosome sample in 25 μl of the buffer were digested with 25 μl of a 0.1 μg $μl^{-1}$ solution of trypsin in 50 mM acetic acid. Samples were digested overnight at 37 °C with slow agitation. The samples were then lyophilized and stored at −80 °C. Immediately prior to analysis, the lyophilized samples were reconstituted with 20 μl aqueous 5% acetonitrile and 0.1% formic acid.

A 6.4 μl aliquot of each digest was analyzed by LC/MS/MS on a Waters/Micromass API US Q-TOF mass spectrometer, interfaced to Waters CapLC. The HPLC system was equipped with a 5 mm × 800 Å i.d. C18 P3 trapping column, and a 15 cm × 75 μm i.d. C18 PepMap analytical column, both from Dionex Corporation. Spectra were acquired in the "survey" mode, where an MS survey scan is acquired first, followed by MS/MS scans on parent ions meeting a preselected intensity threshold. For these experiments, the intensity threshold was set to "1" (the minimum allowable). MS spectra were acquired over the mass range 400–1900, and MS/MS spectra were acquired over the mass range 50–1900, at a scan rate of 1 s per scan.

The Waters/Micromass ProteinLynx software (Version 2.0) was used to create tabulated MS/MS spectra (peak lists) from the raw data. These peak lists were input into a site-licensed version of the Mascot database searching program [29] (www.matrixscience.com), in which we had installed the *L. major* protein and EST databases. The observed MS/MS spectra were matched against spectra from a theoretical digest of all of the proteins in the database.

3. Results

3.1. Release of rRNA-containing RNP particles from L. tarentolae mitochondria

Bacterial and eukaryotic cytoplasmic ribosomes are generally prepared by mechanical disruption of the cells which releases ribosomes that are collected by high speed centrifugation. However, mitochondrial ribosomes are generally strongly associated with the inner membrane of mitochondria and must be released by treatment with detergents. For example, only about half of the ribosomes in mammalian mitochondria are released from membranes by detergent lysis [30].

Preliminary experiments indicated that *L. tarentolae* mitochondrial ribosomes are also strongly associated with the inner membrane. Disruption of isolated mitochondria by repeated cycles of freeze–thawing released less than 20% of the 12S LSU rRNA and only about 30% of the 9S SSU rRNA, as determined by quantitation of the ethidium bromide-stained 9S and 12S bands in polyacrylamide gels (data not shown). Membrane-associated ribosomes from other organisms can usually be released by disrupting electrostatic interactions using high salt and by solubilizing the membranes with detergents. However, even following lysis of *L. tarentolae* mitochondria in 0.5 M KCl, 0.2% NP40, approximately 50% of the 9S rRNA- and 12S rRNA-containing particles remained in the insoluble pellet (data not shown). Furthermore, there was a 1.5–2.0 molar excess of the 9S rRNA over the 12S rRNA, a ratio which differs significantly from the expected 1:1 molar ratio based on the stoichiometry of small and large subunit rRNAs in other systems. This suggests that 9S rRNA complexes may be more abundant in the mitochondrial matrix than 12S rRNA complexes or more stable during isolation. One possible explanation is that, since only

LSU particles normally associate with the inner mitochondrial membrane for the co-translational insertion of nascent polypeptides [31,32], it is likely that these SSU particles are not attached to the membrane during isolation.

In designing an isolation procedure for mitochondrial ribosomes of *L. tarentolae*, we decided to monitor the presence of mitochondrial 9S and 12S rRNAs rather than the total UV-absorbance, due to the known high abundance of non-ribosomal multi-protein UV-absorbing complexes (such as pyruvate dehydrogenase and oligomeric ATPase) which have similar sedimentation values. Solubilization was assayed by several criteria including the yield of rRNP complexes, their intactness (judged by the absence of obvious disassembly products such as individual 12S and 9S rRNAs) and the completeness of membrane solubilization (judged by the lack of smearing across the gradients). In order to determine appropriate membrane solubilization conditions, a number of pilot experiments were performed comparing several non-ionic and zwitterionic detergents (dodecyl maltoside, NP40, Triton X-100, Triton X-114 and CHAPS) in different monovalent and divalent ion concentrations (see Supplementary data). We observed a definite effect of the mitochondrial isolation protocol and freeze–thawing of isolated mitochondria on the nature and reproducibility of the profiles. The protocol selected for further

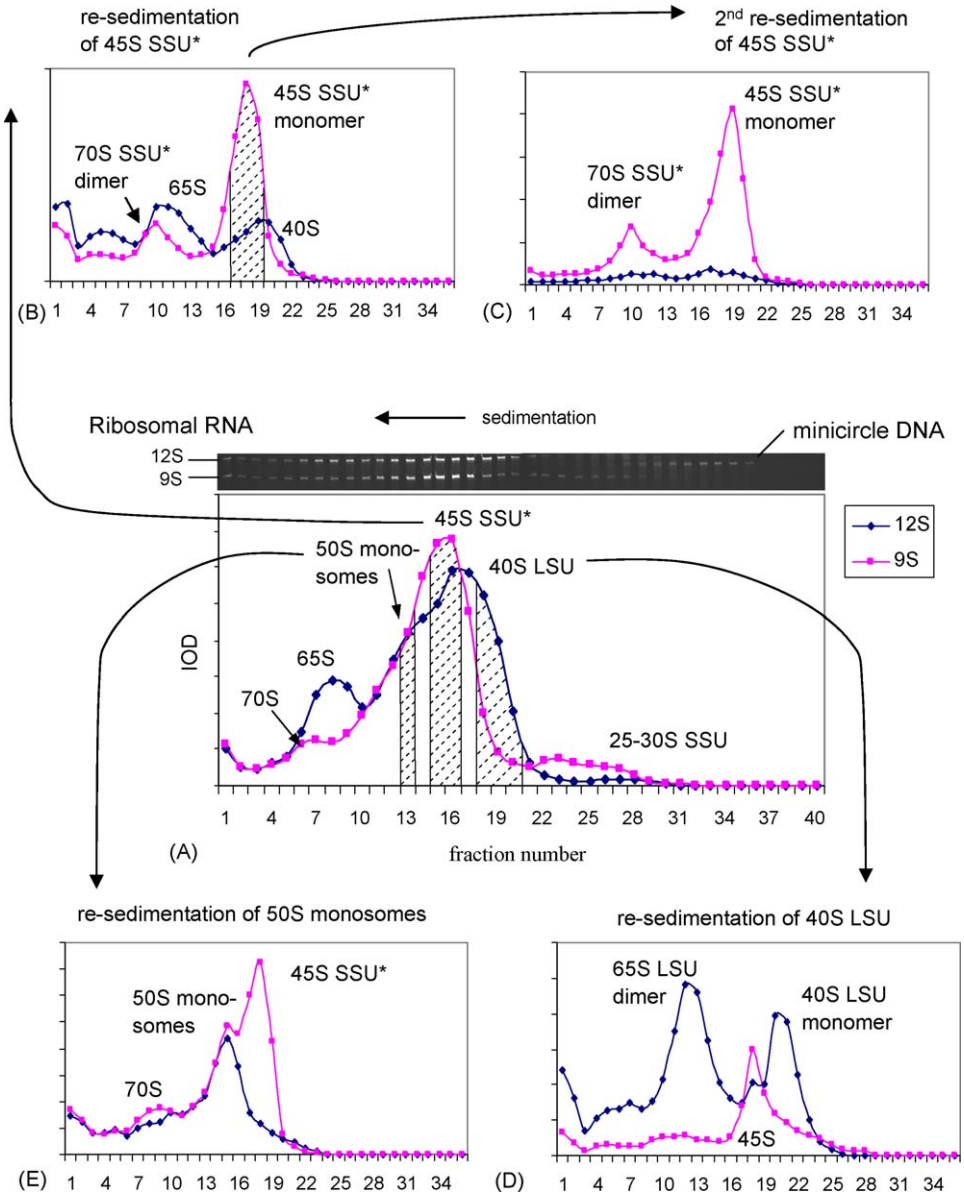

Fig. 1. Gradient centrifugation analysis of individual rRNP complexes: (A) a representative sedimentation profile of the complexes extracted with 2% dodecyl maltoside in 100 mM KCl, 10 mM $MgCl_2$ after puromycin treatment of mitochondria (SW28 rotor, 19,000 rpm, 16 h). The inset panel shows the corresponding electrophoretic gel stained with ethidium bromide. Particles from the fractions enriched with different complexes (indicated by shading) were recovered by pelleting, resuspended in a buffer containing 100 mM KCl (unless indicated otherwise), and sedimented in a second gradient (SW41 rotor, 20,000 rpm, 16 h); (B) particles from fractions 15 and 16 enriched with SSU* 45S complexes; (C) particles obtained from the 45S peak of the gradient in panel (B) after pelleting, treatment with 500 mM KCl and re-sedimentation in a gradient; (D) re-sedimentation of the 40S LSU complexes from the gradient in panel (A), fractions 18–20; (E) 50S monosome complexes from a fraction equivalent to fraction 13 of the gradient in panel (A).

study involved hypotonic cell rupture followed by Percoll density gradient fractionation (see Section 2 and Supplementary data). Mitochondria were used for ribosome isolation directly after isolation and were not frozen. The standard lysis procedure involved treatment of freshly isolated mitochondria with 2 mM puromycin and lysis in 2% dodecyl maltoside, 100 mM KCl, 10 mM $MgCl_2$. By this method, approximately 50% of the rRNPs could be recovered in soluble form.

The sedimentation profile of rRNP complexes released from purified mitochondria by extraction under our standard conditions is shown in Fig. 1A. The majority of the 9S rRNA was present in a particle sedimenting at 45S, with a smaller portion sedimenting around 70S and 30S. The majority of the 12S rRNA sedimented around 40S, with a distinct shoulder at 50S and a minor peak at 65S. The separation of the 50S 12S rRNA-containing particles from the more abundant 45S 9S rRNA-containing particles was small but reproducible.

Insight into the nature of the rRNP complexes observed was obtained by re-sedimentation of fractionated peaks in sucrose gradients, as diagrammed in Fig. 1A. The 45S particles in fractions 15 and 16 in Fig. 1A were recovered by pelleting and subjected to a second gradient fractionation. As shown in Fig. 1B, there was an enrichment of the 45S 9S rRNA-containing peak. The 45S peak fractions 16–19 in Fig. 1B were recovered by pelleting, subjected to treatment with 500 mM KCl and re-sedimented. As shown in Fig. 1C, this led to a near homogeneous preparation of the 9S rRNA-containing 45S and 70S particles. The 45S particles are operationally designated SSU* particles and the 70S particles appear to represent dimers of SSU* particles. Note the almost complete absence of 12S rRNA-containing particles in both preparations. The OD A_{260}/A_{280} ratio of the isolated material in the 45S peak was 0.8 and that suggested a lower RNA to protein ratio in this complex compared to mammalian mitochondrial ribosomes which usually demonstrate the value of 1.2–1.6 (L. Spremulli, unpublished observations).

Re-sedimentation of the 40S 12S rRNA-containing shoulder (fractions 18–20) in Fig. 1A led, as shown in Fig. 1D, to an enrichment for this peak and an increased amount of a 65S 12S rRNA-containing peak. There is now a distinct separation of the 40S 12S rRNA- and the 45S 9S rRNA-containing particles. We present evidence below that the 40S peak represents LSU particles. The 65S peak appears to be due to spontaneous dimerization of the LSU particles produced by the pelleting procedure. The propensity of the 40S LSU particles to aggregate limited further purification by additional successive gradient fractionations.

The 50S shoulder (fraction 13) of 9S and 12S r RNA-containing particles in Fig. 1A was pelleted and re-sedimented in a second sucrose gradient. As shown in Fig. 1E, a distinct 50S peak can be seen, although there is substantial overlapping with the 45S SSU* peak. Due to instability of these particles, several additional successive rounds of pelleting and sedimentation did not succeed in purification of the 50S peak to homogeneity. It is however clear that the 50S fraction represents a discrete complex which is clearly different from the 12S rRNA-containing 40S complex, as well as the 9S rRNA-containing 45S complex. The presence of both the 9S and 12S rRNAs in this complex and additional evidence presented below suggest that the 50S particles represent the ribosomal monosomes.

The minor 9S rRNA-containing 30S peak in Fig. 1A appears somewhat heterogeneous and this was confirmed by re-sedimentation of this region (not shown). The size of these particles and the sole presence of the SSU rRNA indicate that these represent SSU particles.

3.2. Dissociation of the mitochondrial monosomes

A general method to dissociate monosomes in other systems is to lower the Mg^{2+} concentration below 2–3 mM [33]. The protein-rich mitochondrial ribosomes found in other systems usually require in addition high monovalent cation concentration (0.5–1.0 M) for dissociation [34,35]. However, attempts to induce dissociation of the partially purified *L. tarentolae* 50S particles into subunits with 500 mM KCl in 10 mM or 0.1 mM $MgCl_2$ were unsuccessful; the particles appeared to break down with the release of free 12S and 9S rRNA (data not shown). The breakdown was even more pronounced in high salt in the presence of the ionic detergent, deoxycholate (0.2–0.5%). This in vitro behavior is in contrast with the apparent ready dissociation of the 50S particles if mitochondria were lysed in high salt and 2% dodecyl maltoside. As shown in Fig. 2, this procedure yields only two major peaks: the 12S rRNA-containing 40S putative LSU peak and the 9S rRNA-containing 45S SSU* peak. We speculate that the absence of the 30S putative SSU peak is due to a rapid dimerization or modification of these particles forming the 45S SSU* peak, but this must be investigated further.

3.3. Electron microscopy and image analysis of monosomes and subunits

Electron microscopic examination of partially purified 40S, 45S and 50S complexes was performed using negative staining. The 40S particles, which could be well separated from the 45S particles (Fig. 1D), appeared as 20–25 nm particles exhibiting a morphology consistent with their putative LSU designation

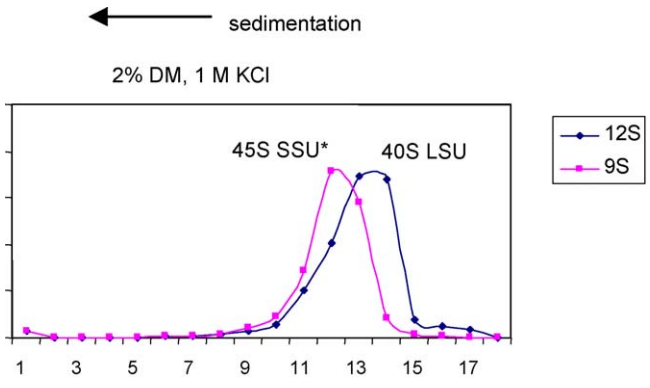

Fig. 2. Sucrose gradient sedimentation analysis of the rRNP complexes extracted from mitochondria of *L. tarentolae* in 2% dodecyl maltoside, 1 M KCl, 10 mM $MgCl_2$. The vertical axis represents integrated optical density of the ethidium bromide-stained RNA, the horizontal axis represents gradient fraction numbers. The sedimentation was from right to left (SW41 rotor, 17,000 rpm, 16 h).

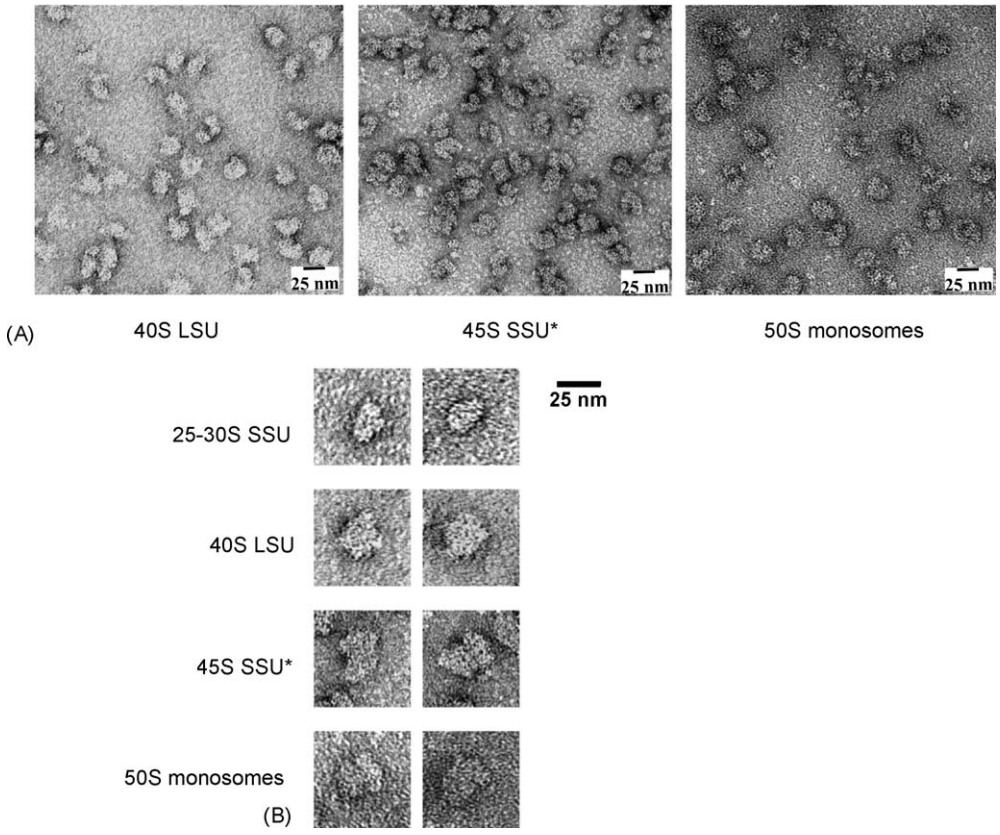

Fig. 3. Negative staining electron microscopy of the rRNP complexes and putative functional designations of the complexes. (A) 40S complexes obtained from a gradient peak similar to fraction 21, Fig. 1D; 45S complexes from fraction 19, Fig. 1C; 50S complexes from fraction 13, Fig. 1A. (B) Representative particles from the corresponding fields shown in panel (A); the 30S particles were from fractions 22 to 27, Fig. 1A, additionally purified by pelleting and centrifugation in a sucrose gradient.

(Fig. 3A). The 30S putative SSU particles, however, could not be separated from cosedimenting oligomeric ATPase complexes, which represented the majority of particles in the examined fields (data not shown). Nonetheless, this preparation also contained particles with morphologies reminiscent of bacterial small subunits (Fig. 3B).

The enigmatic 45S 9S rRNA-containing SSU* particles, which could be purified to near homogeneity (Fig. 1C), appeared as novel particles with two distinct asymmetrical lobes (Fig. 3A and B). These particles do not have the typical appearance of small subunits or monosomes. Rather, they might represent small subunits associated with some other large complexes of a similar size and shape or, perhaps, homodimers of the 30S SSU.

The fraction enriched with the 50S complexes (Fig. 1E) consisted of a heterogeneous population of rRNP particles (Fig. 3A). A large proportion of these particles had an oval appearance with two closely attached lobes, which is reminiscent of bacterial or mitochondrial monosomes (Fig. 3B).

The 50S putative monosome fraction was further investigated by cryo-EM. Two-dimensional averages were calculated by a reference-free alignment of 11,891 particle images. The averages were classified into 87 groups by correspondence analysis. A few representative averages are shown in Fig. 4. A majority (about 62%) of these particle images fall in a group that closely relate to some of the typical views of the *E. coli* 70S ribosomes [37] and mammalian mitochondrial 55S ribosomes [36], with side-by-side placement of SSU and LSU (Figs. 4A and B). The remaining 38% particles include monomers or ribosomal subunits in views that are not usually seen in previous EM studies of ribosomes. Some of these averages appear to be complexes of small and large subunits having additional unidentified masses (Fig. 4C). These unidentified masses appear at the interface side of the subunits and have an overall round shape (marked by an asterisk for the mass attached to the LSU and by two asterisks for the mass attached to the SSU). They do not resemble any known features from two-dimensional averages of a bacterial, cytoplasmic or mammalian mitochondrial SSUs or LSUs [36–38].

These results indicate that several distinct classes of ribosomal complexes are present in *Leishmania* mitochondria. The morphology of the 50S particles, analyzed at a high resolution by cryo-EM, clearly reveals them as the mitochondrial monosomes. The 40S particles showed a morphology, although at a lower resolution, consistent with their representing LSU. The 30S particles are yet poorly characterized but the limited amount of data available is consistent with their SSU designation.

The nature of the 45S SSU* complexes requires additional work but the morphology clearly differs from either monosomes or monomeric subunits.

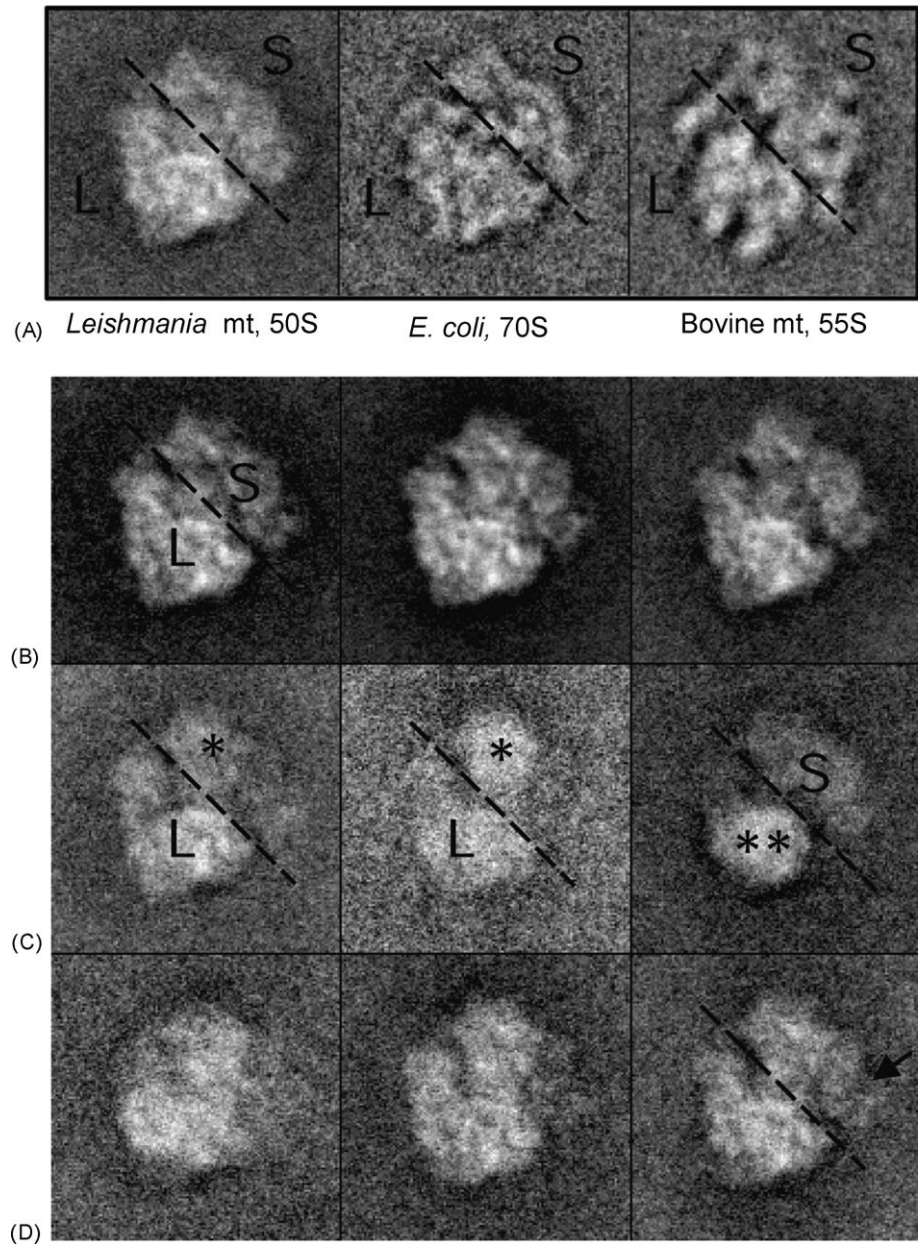

Fig. 4. Two-dimensional averages obtained from cryo-EM images of *L. tarentolae* mitochondrial monosomes in the 50S fraction. (A) Comparison of one of the *L. tarentolae* mitochondrial monosome averages with those of *E. coli* 70S and bovine mitochondrial 55S monosomes. The putative large and small subunits are indicated as L and S, respectively; the two subunits are roughly divided by diagonal dashed line. (B–D) Representative averages of the *L. tarentolae* mitochondrial monosomes: (B) typical monosome-like views, as in panel (A); (C) large and small ribosomal subunits of *L. tarentolae* attached to unidentified globular masses. The first two images show that a globular mass (*) attached to the large subunit, while the third image shows a similar globular mass (**) attached to the small subunit; (D) averages of particles that are only partially matching with the averages shown in rows B and C. The arrow in the last panel points to a significantly weak density area in the small subunit region (compare with averages in row B, and first two averages in row C).

3.4. Detection of SSU and LSU ribosomal protein homologues in the 45S–50S fraction

Tandem mass spectrometry was used to investigate the protein composition of the 45S and 50S particles. A combined 45S–50S fraction (analogous to fractions 13–16 of the gradient in Fig. 1A) was further purified by ion exchange chromatography on Sepharose Q (data not shown). This procedure resulted in a dramatic reduction in contamination by the ATPase and pyruvate dehydrogenase complexes but also resulted in a partial destabilization of the eluted ribosome complexes as was evident from their broad sedimentation profiles when sedimented once again in sucrose gradients (data not shown). This material was digested with trypsin and the peptide mixture was analyzed using nanoscale capillary LC/MS/MS. The product ion spectra were searched versus the non-redundant NCBI database and *Leishmania major* GeneDB database (http://www.genedb.org/genedb/leish/) using the Mascot search program [29]. More than 50 candidate components were identified, including 7 homologs of the SSU ribosomal proteins

Table 1
Homologs of ribosomal proteins identified by the MS/MS analyses of the 45S–50S and 40S complexes

Name	Complexes, *S*-value	*L. major* GeneDB id	NCBI domain (*E* score)	NCBI BLAST hits (*E* score)	Other domains (*E* score)	Size, kDa
MRPS5	45/50	LmjF36.1860	S5 (*E* = 4e−11)	Bacterial S5 (4e−07)	Pfam S5 (6e−02)	49.2
MRPS9	45/50	LmjF23.1190	S9 (*E* = 8e−04)	*Toxoplasma* S9 (0.045)	Pfam S9 (2.1e−02)	39.5
MRPS11	45/50	LmjF05.0340	S11 (*E* = 1e−04)	Bacterial S11 (0.064)	ProDom S11 (0.0004)	40.9
MRPS15	45/50	LmjF20.0510		*S. pombe* MRPS15 (0.003)	ProDom S15 (0.005)	50.2
MRPS16	45/50	LmjF28.0920		*N. crassa* MRPS24/S16 (0.042)	ProDom S16 (0.0003)	22.4
MRPS17	45/50	LmjF35.3850	S17 (*E* = 1e−10)	Bacterial S17 (4e−09)	ProDom S17 (9e−11)	35.9
MRPS18	45/50	LmjF35.2310	S18 (*E* = 0.01)		Pfam S18 (0.72)	37.7
MRPL3	40, 45/50	LmjF29.0030	L3 (2e−15)	Mitochondrial L3 (2e−28)		53.9
MRPL4	40, 45/50	LmjF11.1360			SCOP: L4 fold (4e−07)	49.9
MRPL7/L12	40	LmjF14.0150	L7/L12 (7e−08)	Mitochondrial and bacterial L7/L12 (1e−09)		19.5
MRPL11	40	LmjF22.2220	L11 (1e−14)	Mitochondrial and bacterial L11 (1e−11)		40.2
MRPL15	45/50	LmjF16.0010	L15 (1e−05)	Mitochondrial L15 (4e−08)		43.5
MRPL16	40	LmjF14.0950	L16 (9e−08)	Mitochondrial and bacterial L16 (2e−06)		19.1
MRPL21	40, 45/50	LmjF14.0780	L21 (9e−17)	Mitochondrial and bacterial L21 (1e−09)		21.0
MRPL23	45/50	LmjF25.0890			Pfam: L23 (2.2e−02)	28.7
MRPL28	40, 45/50	LmjF30.2750		Mitochondrial L28 (0.57)		27.1
MRPL30	40	LmjF04.0860		Archeal L30 (0.28)	SCOP: L30 fold (6e−11), transmembrane	45.4
MRPL43	45/50	LmjF31.1550	L51/S25/CI-B8 (8e−06)	*Drosophila* MRPL43 (2e−06)	ProDom L43 (2e−06)	31.1
MRPL46	40	LmjF06.0040		Mouse MRPL46 (2e−08)	ProDom L30 (7e−08)	33.2
MRPL47	40, 45/50	LmjF04.0270	MRPL47 (8e−24)	Mitochondrial L47 (2e−09)		54.1

(MRPS5, MRPS9, MRPS11, MRPS15, MRPS16, MRPS17 and MRPS18) and 9 homologs of the LSU proteins (MRPL3, MRPL4, MRPL15, MRPL21, MRPL23, MRPL28, MRPL43, MPRL46 and MRPL47) from other organisms (Table 1).

Since the digested material involved a mixture of two 45S and 50S particles, it was not possible to assign the identified polypeptides to a specific particle based on this experiment. However, a recent analysis of a highly purified 45S SSU* fraction has shown these particles contain only SSU ribosomal proteins in addition to proteins which do not have homologs among known ribosomal proteins (data not shown). Therefore, the LSU ribosomal protein homologs must have originated from the 50S putative monosome particles. Additional analyses are needed to ascertain the authenticity of the components with no homologs in other ribosomes, as well as to search for any potential missing ribosomal proteins.

3.5. Detection of large subunit ribosomal protein homologues in the 40S putative LSU particles

As discussed above, re-sedimentation of enriched 40S fractions led to apparent dimerization and formation of a 65S peak (Fig. 1D). Since this peak was relatively free of contamination with the 45S SSU* peak or with F_1F_0 ATPase or cytochrome *c* oxidase, it was selected for proteomics analysis by ESI/MS/MS. Analysis revealed the presence of 11 homologs of the known LSU proteins MRPL3, MRPL4, MRPL7/L12, MRPL11, MRPL16, MRPL21, MRPL28, MRPL30, MRPL43, MRPL46 and MRPL47 (Table 1). No homologs of SSU proteins were detected. Additional novel proteins were also found, but it remains to be determined whether or not these polypeptides are components of the 40S LSU particles. These findings, however, confirm the designation of the 40S particle as the LSU.

4. Discussion

Several rRNA-containing rRNP particles have been identified in mitochondrial lysates from *L. tarentolae*: (1) a 40S particle that contains only the LSU rRNA and LSU protein homologs, and has a morphology characteristic of LSU particles from other organisms; (2) a 50S particle that contains both LSU and SSU rRNAs, LSU protein homologs (and probably also SSU homologs), and has a morphology characteristic of monosomes from other organisms; (3) a 30S particle that contains only SSU rRNA; (4) a 45S particle that contains only SSU rRNA and has only SSU protein homologs; (5) a 65S particle that contains only LSU rRNA and represents an apparent dimer of the 40S particle; (6) a 70S particle that contains only SSU rRNA and represents an apparent dimer of the 45S particle.

Although a detailed characterization of the 50S particles awaits their purification to homogeneity, the evidence obtained indicates that these particles represent the trypanosomatid mitochondrial ribosomes. Most importantly, abundant monosome-like particles were found in the 50S fraction and their identification was confirmed by a high-resolution cryo-electron microscopy (Fig. 4). Moreover, this gradient fraction corresponds to a peak of poly(U)-directed phenylalanine polymerization activity observed using pre-charged *E. coli* Phe-tRNA and a detergent extract of *L. tarentolae* mitochondria as a source of elongation factors (L. Spremulli, unpublished results). A second peak of poly(U)-directed phenylalanine polymerization activity corresponds to a region of the gradient enriched about two-fold in the LSU rRNA over the SSU rRNA (corresponds to fraction 19 in Fig. 1A).This fraction is likely to contain a mixture of ribosomal subunits which associate during the reaction.

The interpretation that the 50S complexes represent monosomes is also consistent with the finding that these particles are

relatively labile compared to the 45S and 40S particles, apparently breaking apart upon lysis of the mitochondria in 500 mM KCl. The observed lack of dissociation of the isolated 50S monosome complexes in vitro could be due to the lack of specific dissociation-promoting factors.

The 40S particle appears to represent the LSU. This complex has a shape reminiscent of bacterial LSU particles and contains only LSU rRNA and several homologs of LSU proteins. The situation with regard to the SSU is complicated by the presence of abundant stable 45S SSU* particles containing only SSU rRNA and only SSU protein homologues. The size of these particles is not consistent with them representing the SSU, in view of the size and morphology of the 50S monosome. In addition, attempts to induce the association of purified 45S SSU* and 40S LSU complexes in vitro resulted only in the formation of small amounts of the 65S and 70S homodimer complexes (data not shown).

The minor SSU rRNA-containing peak at 30S could represent the SSU. Additional characterization of the 30S complexes is necessary, but their size and morphology are consistent with their designation as the SSU particle. The question remains, however, why dissociation of the 50S monosome does not produce free 30S particles but rather 40S LSU particles and 45S SSU* particles. The 45S particles may represent a form of in vitro sequestration of the individual small subunits either by oligomerization and/or combination with additional proteins. The latter possibility is suggested by a recent proteomics analysis of these particles which shows more than 40 polypeptides with a combined molecular mass exceeding 2.2 MDa (D.A. Maslov, A.M. Falick, L.L. Spremulli, L. Simpson, unpublished results), almost twice as much as can be expected for a small subunit (see e.g. [36–38]). Purification of these complexes to homogeneity and additional analyses are required to resolve relationships among them.

Acknowledgments

D. Maslov is very thankful to the members of the Simpson lab for their hospitality during his sabbatical stay. We thank T. Booth and M. Breedlove for help with cryo-EM and image processing, respectively. We also thank J. Lake and R. Aphasizhev for discussions and M. Peris and S. Wilkens for help with conventional transmission electron microscopy at the initial stages of this project. This work was supported in part by NIH grants AI09102 (to L.S.), GM32734 (to L.L.S.) and GM61576 (to R.K.A.) and an HFSP grant RGY232003 (to R.K.A.). This study was also partially funded by a gift from an anonymous donor to support research in proteomics at the University of North Carolina.

Appendix A. Supplementary data

Supplementary data associated with this article can be found, in the online version, at doi:10.1016/j.molbiopara.2006.02.021.

References

[1] Feagin JE. Mitochondrial genome diversity in parasites. Int J Parasitol 2000;30:371–90.
[2] Lukeš J, Guilbride DL, Votýpka J, Zíková A, Benne R, Englund PT. Kinetoplast DNA network: evolution of an improbable structure. Eukaryot Cell 2000;1:495–502.
[3] Shlomai J. The structure and replication of kinetoplast DNA. Curr Mol Med 2004;4:623–47.
[4] Simpson L, Aphasizhev R, Gao G, Kang X. Mitochondrial proteins and complexes in *Leishmania* and *Trypanosoma* involved in U-insertion/deletion RNA editing. RNA Publ RNA Soc 2004;10:159–70.
[5] Simpson L, Sbicego S, Aphasizhev R. Uridine insertion/deletion RNA editing in trypanosome mitochondria: a complex business. RNA Publ RNA Soc 2003;9:265–76.
[6] Stuart KD, Panigrahi AK, Salavati R. RNA editing in kinetoplastid mitochondria. In: Bass BL, editor. RNA editing. Oxford University Press; 2001. p. 1–19.
[7] Aphasizhev R, Aphasizheva I, Nelson RE, et al. Isolation of a U-insertion/deletion editing complex from *Leishmania tarentolae* mitochondria. EMBO J 2003;22:913–24.
[8] Blum B, Bakalara N, Simpson L. A model for RNA editing in kinetoplastid mitochondria: "Guide" RNA molecules transcribed from maxicircle DNA provide the edited information. Cell 1990;60:189–98.
[9] Kable ML, Seiwert SD, Heidmann S, Stuart K. RNA editing: a mechanism for gRNA-specified uridylate insertion into precursor mRNA. Science 1996;273:1189–95.
[10] McManus MT, Shimamura M, Grams J, Hajduk SL. Identification of candidate mitochondrial RNA editing ligases from *Trypanosoma brucei*. RNA Publ RNA Soc 2001;7:167–75.
[11] Rusché LN, Cruz-Reyes J, Piller KJ, Sollner-Webb B. Purification of a functional enzymatic editing complex from *Trypanosoma brucei* mitochondria. EMBO J 1997;16:4069–81.
[12] Horváth A, Berry EA, Maslov DA. Translation of the edited mRNA for cytochrome *b* in trypanosome mitochondria. Science 2000;287:1639–40.
[13] Horváth A, Kingan TG, Maslov DA. Detection of the mitochondrially encoded cytochrome *c* oxidase subunit I in the trypanosomatid protozoan *Leishmania tarentolae*. J Biol Chem 2000;275:17160–5.
[14] Horváth A, Neboháčová M, Lukeš J, Maslov DA. Unusual polypeptide synthesis in the kinetoplast–mitochondria from *Leishmania tarentolae*. Identification of individual de novo translation products. J Biol Chem 2002;277:7222–30.
[15] Neboháčová M, Maslov DA, Falick AM, Simpson L. The effect of RNA interference down-regulation of RNA editing 3′-terminal uridylyl transferase (TUTase) 1 on mitochondrial de novo protein synthesis and stability of respiratory complexes in *Trypanosoma brucei*. J Biol Chem 2004;279:7819–25.
[16] de la Cruz V, Neckelmann N, Simpson L. Sequences of six structural genes and several open reading frames in the kinetoplast maxicircle DNA of *Leishmania tarentolae*. J Biol Chem 1984;259:15136–47.
[17] Eperon I, Janssen J, Hoeijmakers J, Borst P. The major transcripts of the kinetoplast DNA of *T. brucei* are very small ribosomal RNAs. Nucleic Acids Res 1983;11:105–25.
[18] de la Cruz V, Lake JA, Simpson AM, Simpson L. A minimal ribosomal RNA: Sequence and secondary structure of the 9S kinetoplast ribosomal RNA from *Leishmania tarentolae*. Proc Natl Acad Sci USA 1985;82:1401–5.
[19] de la Cruz V, Simpson A, Lake J, Simpson L. Primary sequence and partial secondary structure of the 12S kinetoplast (mitochondrial) ribosomal RNA from *Leishmania tarentolae*: conservation of peptidyl-transferase structural elements. Nucleic Acids Res 1985;13:2337–56.
[20] Chugunov VA, Shirshov AT, Zaitseva GN. A comparative study of the ribosomes from kinetoplasts and cytoplasm of the zooflagellate, *Strigomonas oncopelti*. Biokhimiya 1971;36:630–5 [in Russian].
[21] Hanas J, Linden G, Stuart K. Mitochondrial and cytoplasmic ribosomes and their activity in blood and culture form *Trypanosoma brucei*. J Cell Biol 1975;65:103–11.
[22] Shu HH, Göringer HU. *Trypanosoma brucei* mitochondrial ribonucleoprotein complexes which contain 12S and 9S ribosomal RNAs. Parasitology 1998;116:157–64.
[23] Tittawella I, Yasmin L, Baranov V. Mitochondrial ribosomes in a trypanosome. Biochem Biophys Res Commun 2003;307:578–83.

[24] Braly P, Simpson L, Kretzer F. Isolation of kinetoplast–mitochondrial complexes from *Leishmania tarentolae*. J Protozool 1974;21:782–90.
[25] Wagenknecht T, Grassucci R, Frank J. Electron microscopy and computer image averaging of ice-embedded large ribosomal subunits from *Escherichia coli*. J Mol Biol 1988;199:137–47.
[26] Frank J, Bretaudiere JP, Carazo JM, Verschoor A, Wagenknecht T. Classification of images of biomolecular assemblies: a study of ribosomes and ribosomal subunits of *Escherichia coli*. J Microsc 1988;150(Pt 2):99–115.
[27] Frank J, Radermacher M, Penczek P, et al. SPIDER and WEB: processing and visualization of images in 3D electron microscopy and related fields. J Struct Biol 1996;116:190–9.
[28] Bienvenut WV, Deon C, Pasquarello C, et al. Matrix-assisted laser desorption/ionization-tandem mass spectrometry with high resolution and sensitivity for identification and characterization of proteins. Proteomics 2002;2:868–76.
[29] Perkins DN, Pappin DJ, Creasy DM, Cottrell JS. Probability-based protein identification by searching sequence databases using mass spectrometry data. Electrophoresis 1999;20:3551–67.
[30] Liu MQ, Spremulli L. Interaction of mammalian mitochondrial ribosomes with the inner membrane. J Biol Chem 2000;275:29400–6.
[31] Herrmann JM, Neupert W. Protein insertion into the inner membrane of mitochondria. IUBMB Life 2003;55:219–25.
[32] Stuart R. Insertion of proteins into the inner membrane of mitochondria: the role of the *Oxa*1 complex. Biochim Biophys Acta 2002;1592:79–87.
[33] Zitomer RS, Flaks JG. Magnesium dependence and equilibrium of the *Escherichia coli* ribosomal subunit association. J Mol Biol 1972;71:263–79.
[34] Matthews DE, Hessler RA, Denslow ND, Edwards JS, O'Brien TW. Protein composition of the bovine mitochondrial ribosome. J Biol Chem 1982;257:8788–94.
[35] Spedding G. Isolation and analysis of ribosomes from prokaryotes, eukaryotes and organelles. In: Spedding G, editor. Ribosomes and protein synthesis—a practical approach. IRL Press; 1990. p. 1–29.
[36] Gabashvili IS, Agrawal RK, Spahn CM, et al. Solution structure of the *E. coli* 70S ribosome at 11.5 Å resolution. Cell 2000;100:537–49.
[37] Sharma MR, Koc EC, Datta PP, Booth TM, Spremulli LL, Agrawal RK. Structure of the mammalian mitochondrial ribosome reveals an expanded functional role for its component proteins. Cell 2003;115:97–108.
[38] Spahn CM, Beckmann R, Eswar N, et al. Structure of the 80S ribosome from *Saccharomyces cerevisiae*—tRNA–ribosome and subunit–subunit interactions. Cell 2001;107:373–86.